Escherichia coli Proline tRNA Synthetase Is Sensitive to Changes in the Core Region of $tRNA^{Pro}$ †

Hongjian Liu and Karin Musier-Forsyth*

Department of Chemistry, University of Minnesota, Minneapolis, Minnesota 55455

Received June 10, 1994; Revised Manuscript Received August 9, 1994®

ABSTRACT: To investigate the relationship between tRNA conformation and specific recognition by aminoacyl-tRNA synthetases, a full-length tRNA molecule was assembled by annealing together two oligonucleotides representing fragments of *Escherichia coli* $tRNA^{Pro}$. A shorter chemically synthesized 5′-fragment (7–18 nucleotides) was combined with an *in vitro* transcribed 3′-fragment (59 nucleotides). Despite a break in the phosphodiester backbone between nucleotides U17a and G18, this tRNA molecule was an efficient substrate for class II *Escherichia coli* proline tRNA synthetase. While the deletion of three D-loop nucleotides (U17a, U17, and C16) was tolerated, removal of G15 and A14 significantly reduced aminoacylation efficiency. Hybrid DNA–RNA "annealed" substrates were also prepared and assayed for aminoacylation. Native gel electrophoresis was used to compare the global folding of the various substrates tested. The results of these studies suggest that proline tRNA synthetase is sensitive to changes in the core region of $tRNA^{Pro}$ through which information required for efficient aminoacylation may be transmitted. In particular, nucleotides in the D-loop and backbone functional groups in the D-stem appear to be critical for maintaining a tRNA structure that is optimal for recognition by proline tRNA synthetase *in vitro*.

Aminoacyl-tRNA synthetases catalyze a two-step reaction that results in the esterification of specific amino acids onto the 3′-end of tRNA molecules. In the first step, an enzyme-bound complex between ATP and the amino acid, known as the aminoacyl-adenylate, is formed. The amino acid is transferred to the tRNA molecule in the second step of the reaction. The proteins that catalyze these reactions are divided into 2 classes of 10 enzymes each on the basis of conserved sequence motifs (Schimmel, 1987; Cusack et al., 1990; Eriani et al., 1990).

It is widely believed that all tRNAs fold into a similar L-shaped tertiary structure (Giegé et al., 1993). The crystal structure of $tRNA^{Phe}$ shows that nine conserved tertiary interactions make up the central core of the tRNA molecule and are responsible for its three-dimensional fold (Kim et al., 1974). Despite structural similarities between tRNAs, each synthetase must recognize its cognate tRNA substrate and discriminate among the other noncognate tRNAs. Therefore, while the three-dimensional structure of all tRNA molecules is similar, subtle differences in tRNA structural elements are likely to exist. Recent evidence that tRNAs differ in structure comes from experiments using probes of DNA structure (Chow & Barton, 1990, 1992; Chow et al., 1992; Holmes et al., 1993). These probes are able to distinguish small differences in the three-dimensional structures of tRNA molecules that may play a role in their specific interactions with aminoacyl-tRNA synthetases.

The relationship between tRNA conformation and synthetase recognition is difficult to examine directly. In the limited number of experiments that have been performed to address this question to date, different effects have been seen. For example, elements of the central core are an important part of the recognition of *Escherichia coli* $tRNA^{Phe}$ by phenylalanine tRNA synthetase (Peterson & Uhlenbeck, 1992). Recent results suggest that a tertiary interaction also plays a role in *E. coli* $tRNA^{Cys}$ recognition by its cognate class I synthetase (Hou et al., 1993; Hou, 1994). Yeast phenylalanine tRNA synthetase, on the other hand, is relatively insensitive to modifications that introduce foreign tertiary interactions into its tRNA substrate (Sampson et al., 1990). Moreover, while yeast aspartyl-tRNA synthetase can efficiently catalyze the aspartylation of a $tRNA^{Asp}$ transcript containing $tRNA^{Phe}$ conformational features (Perret et al., 1990), the maintenance of a base-paired D-stem is required for this enzyme (Puglisi et al., 1993).

Additive, cooperative, and anticooperative effects between "identity" nucleotides of $tRNA^{Asp}$ have also been seen (Pütz et al., 1993). "Identity" elements are nucleotides that direct and modulate specific aminoacylation by aminoacyl-tRNA synthetases (McClain, 1993; Saks et al., 1994). The amino acid acceptor stem and the anticodon loop are the two regions of the tRNA with the highest density of these recognition elements. However, the mechanism for information transfer between these distal tRNA domains is not clear. A study of $minihelix^{Val}$ aminoacylation (Frugier et al., 1992) suggested that information originating from the anticodon stem–loop can be transmitted to the active site of the enzyme by the core of the protein. In this system, an acceptor stem minihelix is aminoacylated weakly, and the signal is stimulated in the presence of a separate anticodon stem–loop minihelix. Minihelices, however, are not substrates for *E. coli* proline tRNA synthetase (ProRS),[1] and aminoacylation of an acceptor stem $minihelix^{Pro}$ cannot be specifically induced by a separate anticodon stem–loop minihelix (H. Liu and K. Musier-Forsyth,

† This work was funded by Grant GM49928 from the National Institutes of Health. Acknowledgment is also made to the donors of The Petroleum Research Fund, administered by the American Chemical Society, and to the American Cancer Society (Grant IN-13-33-15) for partial support of this research.

* To whom correspondence should be addressed at the Department of Chemistry, University of Minnesota, 207 Pleasant St. S.E., Minneapolis, MN 55455. Telephone: (612) 624-0286. FAX: (612) 626-7541. e-mail: musier@chemsun.chem.umn.edu.

® Abstract published in *Advance ACS Abstracts,* September 15, 1994.

[1] Abbreviations: ProRS, proline-tRNA synthetase; FPLC, fast protein liquid chromatography; SDS, sodium dodecyl sulfate; HEPES, 4-(2-hydroxyethyl)-1-piperazineethanesulfonic acid.

0006-2960/94/0433-12708$04.50/0

unpublished results). This suggests indirectly that the core of the tRNA molecule may be important for transmitting information that is important for aminoacylation by ProRS.

In order to improve our understanding of the role of tRNA conformation on discrimination by aminoacyl-tRNA synthetases, we developed a fragment approach to study tRNA recognition by ProRS. *Escherichia coli* proline tRNA synthetase is a dimer of identical subunits with a total molecular mass of 127 kDa (Eriani et al., 1990). All three of the conserved sequence motifs that define class II synthetases have been identified in the primary sequence of this enzyme (Eriani et al., 1990). An *in vivo* study showed that ProRS uses nucleotides in both the acceptor stem and the anticodon loop to recognize its cognate tRNA (McClain et al., 1994). Site-directed mutagenesis of full-length tRNA^{Pro} molecules prepared by *in vitro* transcription has recently been carried out and supports this conclusion (H. Liu, R. Peterson, J. Kessler, and K. Musier-Forsyth, unpublished results). The ability to reconstruct an active tRNA molecule from RNA fragments obtained from enzymatic or chemical cleavage of an intact tRNA has been previously demonstrated (Imura et al., 1969; Thiebe & Zachau, 1969; Thiebe et al., 1972; Fittler & Zachau, 1973; Wübbeler et al., 1975). In a more recent study, base-substituted synthetic oligoribonucleotides were combined with a 3/4 tRNA^{Gln} molecule to investigate the role of base functional groups in *E. coli* tRNA^{Gln} identity (Hayase et al., 1992). In the present work, we combine chemically synthesized RNA oligonucleotides corresponding to the 5′-7–18 nucleotides of tRNA^{Pro} with a 3′-3/4 tRNA^{Pro} fragment synthesized by *in vitro* transcription. Both base and backbone modifications are incorporated into the synthetic portion of the reconstructed tRNA^{Pro} molecule. The results suggest that maintenance of the core region of tRNA^{Pro} is required for efficient aminoacylation with proline and that ProRS is particularly sensitive to changes that alter the structure of the D-stem.

MATERIALS AND METHODS

Protein Purification and Assays. *E. coli* SY327 carrying two plasmids, pGT1–2 and pGT1–2#, was a gift from Mike Syvaney. pGT1–2 contains the T7 RNA polymerase gene under the heat-inducible λP_L promoter. pGT1–2# contains the ProRS gene under a T7 RNA polymerase promoter. To prepare ProRS using this double-plasmid expression system, *E. coli* SY327 carrying the constructs was grown in 4 L of Luria Bertani (LB) media at 30 °C to an OD_{600} of about 0.5. The cells were induced by growing at 42 °C for an additional 8 h. All subsequent steps were carried out at 4 °C. Cells (25–30 g wet weight) were harvested by centrifugation and resuspended in 5 mL/g of wet cells of resuspension buffer [50 mM K_2HPO_4 (pH 7.5)/100 mM NaCl/4 mM EDTA/50 mM β-mercaptoethanol]. Protease inhibitors (1 mM benzamidine, 40 μg/mL leupeptin, 20 μg/mL aprotinin, 4 μg/mL pepstatin, and 0.1%/volume of a saturated 2-isopropanol solution of phenylmethanesulfonyl fluoride) were freshly prepared and immediately added to the resuspended cells. Cells were lysed by sonication and spun at 29 000 rpm in a fixed-angle rotor of a Beckman ultracentrifuge for 1 h. The supernatant was mixed slowly on ice with 243 g/L of "enzyme grade" ammonium sulfate (0–40% cut). After 15 min of gentle stirring, the precipitate was collected by centrifugation (10000*g* for 10 min) and discarded. Ammonium sulfate was slowly added to the supernatant (63 g/L, 40–60% cut) as described above. Following centrifugation, the pellet was resuspended in 5–10 mL of buffer A [50 mM K_2HPO_4 (pH 7.5)/2 mM β-mercaptoethanol], put into standard cellulose dialysis tubing (12 000–14 000 MW cutoff), and dialyzed overnight against the same buffer. The sample was clarified by centrifugation and filtration through a 0.22 μm syringe filter and loaded onto a HiLoad (26/10) Q-Sepharose Fast Flow FPLC anion exchange column (Pharmacia) equilibrated in buffer A. The sample was washed with 3 column volumes of buffer A at a flow rate of 5 mL/min. The bound protein was eluted by application of a 800 mL gradient of NaCl from 0 to 300 mM in buffer A. The peak fractions were detected by SDS–polyacrylamide gel electrophoresis (8%) and eluted at about 180 mM NaCl. Peak fractions were pooled and concentrated either by ultrafiltration using Centricon 30 (Amicon) concentrators or by ammonium sulfate precipitation. The partially purified protein (3 mL) was then applied to a HiLoad (16/60) Superdex 200 prep grade FPLC sizing column (Pharmacia) preequilibrated in 50 mM HEPES (pH 7.5)/100 mM NaCl/2 mM β-mercaptoethanol. The sample was eluted with 124 mL of the same buffer at a flow rate of 1 mL/min. Peak fractions were again detected by SDS gel electrophoresis, pooled, and concentrated using Centricon 30 (Amicon) concentrators. For final storage at −20 °C, the protein was put into 25–50 mM K_2HPO_4 (pH 7.5)/2 mM dithiothreitol/40% glycerol. The above purification routinely yielded 150 mg of ProRS that was judged to be >95% pure by SDS–polyacrylamide gel electrophoresis.

ProRS protein concentrations were based on active-site titrations using the adenylate burst assay (Fersht et al., 1975). Aminoacylation assays were conducted at 25 °C in a reaction mixture containing 50 mM HEPES, pH 8.0, 20 mM KCl, 25 mM $MgCl_2$, 20 mM β-mercaptoethanol, 0.1 mg/mL bovine serum albumin, 22.9 μM [^{3}H]proline, 4 mM ATP, 50 nM ProRS, and 0.5–12 μM tRNA or annealed tRNA substrates. At desired time intervals, reaction aliquots were spotted onto TCA-soaked Whatman 3MM filter pads and washed as previously described (Jasin et al., 1985). The specific activity (cpm per picomoles of proline) of the assay mix was determined by spotting 4 μL of reaction cocktail onto Whatman 3MM filter pads without washing. To correct for the unequal quenching of free versus tRNA-bound [^{3}H]proline precipitated onto the filter pads, specific activities determined using free proline were multiplied by a factor of 6.7 for assays of full-length tRNA and 5.8 for assays using the annealed 3′- and 5′-fragments. These ^{3}H quenching factors were determined by performing some assays with ^{14}C-labeled proline.

T7 RNA polymerase was purified according to Grodberg and Dunn (1988) from *E. coli* strain BL-21/pAR 1219 that was a gift of F. William Studier.

Ribonucleic Acids. To facilitate the preparation of large quantities of unmodified tRNA^{Pro} by *in vitro* transcription, the gene for the UGG isoacceptor (Sprinzl et al., 1989) was assembled by cloning a set of six overlapping synthetic DNA oligonucleotides into the *Eco*RI and *Bam*HI sites of pUC119 (Sampson & Uhlenbeck, 1988). The upstream consensus promoter of T7 RNA polymerase and a downstream *Bst*NI restriction site were also introduced into the plasmid. Because all *E. coli* tRNA^{Pro} isoacceptor sequences begin with a 5′-cytidine nucleotide and T7 RNA polymerase requires a guanosine at position 1 for efficient template transcription, the 5′-cytidine nucleotide of tRNA^{Pro} was *not* encoded in the full-length gene construct. The tRNA molecule transcribed using this plasmid, therefore, lacks the first nucleotide and is designated as ΔC1 tRNA^{Pro}. A construct encoding the 3′-59 nucleotides of tRNA^{Pro} in front of a T7 RNA polymerase promoter was similarly prepared. *Bst*NI linearized DNA was then used to prepare *in vitro* run-off full-length ΔC1 and 3/4 tRNA^{Pro} transcripts using established procedures (Milligan

et al., 1987; Shi et al., 1990). RNA transcripts were purified on 12% polyacrylamide gels. Before storage at −20 °C, full-length ΔC1 tRNA^{Pro} was taken up in 10 mM Tris-HCl/1 mM EDTA (pH 8.0) and renatured by heating to 80 °C for 2–3 min. The mixture was transferred to a 60 °C water bath for 2 min, and then $MgCl_2$ was added to 10 mM. The mixture was brought to room temperature over a period of a few minutes and finally placed on ice. The 59-nucleotide 3′-fragment was stored in 10 mM Tris-HCl/1 mM EDTA (pH 8.0) at −20 °C without prior annealing. Immediately prior to the aminoacylation assays, the 5′- and 3′-fragment molecules were annealed as follows. The fragments were combined in a ratio of 1:1.5 (excess 5′-oligomer) in 50 mM HEPES and heated at 60 °C for 3 min. $MgCl_2$ was then added to 10 mM, and the mixture was cooled to room temperature for a few minutes and finally placed on ice.

Synthetic DNA, RNA, and mixed RNA–DNA oligonucleotides were prepared by chemical synthesis on a Gene Assembler Plus (Pharmacia) using the phosphoramidite method (Scaringe et al., 1990). Oligonucleotides were purified on 16% polyacrylamide gels.

For the determination of RNA concentrations, the following extinction coefficients were employed: full-length annealed tRNA, 60.4×10^4 M^{-1}; 59-mer, 47×10^4 M^{-1}; 18-mer, 14×10^4 M^{-1}; 17-mer, 13.5×10^4 M^{-1}; 16-mer, 13×10^4 M^{-1}; 15-mer, 12×10^4 M^{-1}; 14-mer, 11.5×10^4 M^{-1}; 13-mer, 10.7×10^4 M^{-1}; 7-mer, 6.5×10^4 M^{-1}. These values were determined experimentally as described previously (Musier-Forsyth et al., 1991).

Native Polyacrylamide Gel Electrophoresis. Gels were 2 mm thick and consisted of a 30 cm long resolving gel containing 12% acrylamide (29:1 mono:bis), 25 mM Tris/0.12 mM glycine (pH 7.4), and 10 mM $MgCl_2$. A 10 cm stacking gel contained 5% acrylamide (29:1 mono:bis), 25 mM Tris/0.12 mM glycine (pH 5.8), and 10 mM $MgCl_2$. Following annealing using the protocols described above, glycerol was added to each sample to a final concentration of 40%. Approximately 5.6 μg of annealed tRNA was applied to each lane. The gels were run overnight in a 4 °C cold room and stained with ethidium bromide for visualization.

RESULTS

To facilitate this investigation, a tRNA^{Pro} molecule was prepared from two fragment molecules as shown in Figure 1. Maximum activity of the annealed fragments was achieved when they were heated together at 60 °C for 3 min, followed by the addition of Mg^{2+} to 10 mM and slow cooling to room temperature. Under these conditions, reproducible results were obtained for all of the fragments tested. While the 3′-3/4 tRNA alone was not aminoacylated, upon annealing to the 5′-18-mer, efficient aminoacylation could be achieved (Figure 2). Furthermore, ligation of the phosphodiester bond between positions U17a and G18 was not required for activity. While native *E. coli* tRNA^{Pro} has not been purified or tested for aminoacylation by ProRS, we have determined the kinetic parameters for aminoacylation of an unmodified *in vitro*-synthesized tRNA^{Pro} transcript that lacks the first C (ΔC1). The C at position 1 has been deleted to facilitate *in vitro* transcription. The K_M for this substrate is 4.2 μM, and the k_{cat} is 0.27 s^{-1}. A k_{cat}/K_M of 9.0×10^{-3} s^{-1}·μM^{-1} for the annealed transcript was also determined. The specificity constant (k_{cat}/K_M) for aminoacylation of the annealed molecule was, therefore, reduced approximately 7-fold relative to the full-length ΔC1 *in vitro* transcript. Individual values for k_{cat} and K_M were estimated to be 0.060 s^{-1} and 6.7 μM, respectively, for the annealed substrate. A slightly elevated

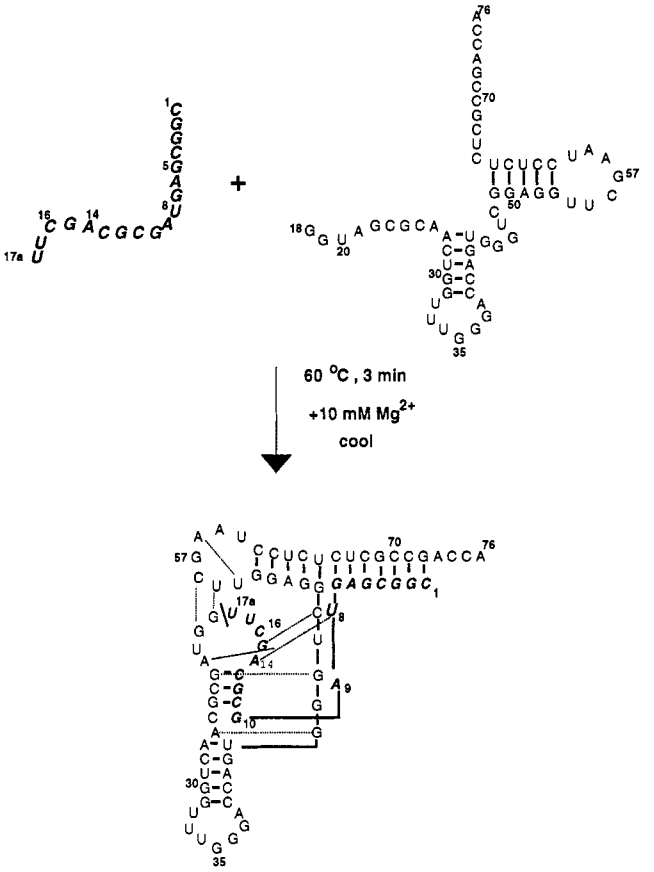

FIGURE 1: Scheme showing the nucleotide sequence and preparation of *E. coli* tRNA^{Pro} from two fragments. A 5′-18-mer oligonucleotide (upper left, bold, italics) was prepared by automated chemical RNA synthesis and combined with an *in vitro*-transcribed 3′-59-mer (upper right). The two fragments were heated at 60 °C in 50 mM HEPES, pH 8.0, for 3 min. $MgCl_2$ (10 mM) was added, and the mixture was allowed to cool to room temperature. The product is shown in the folded L-shaped representation with the break in the phosphodiester backbone between the two fragments indicated by a solid line between U17a and G18. Tertiary interactions are represented by dotted lines and are based on the known structure of tRNA^{Phe}.

K_M and a 4.5-fold reduced k_{cat} were, therefore, both factors in the reduction in aminoacylation efficiency.

Since a break in the phosphodiester backbone of tRNA^{Pro} in the D-loop between U17a and G18 is tolerated by ProRS, we used a deletion analysis to probe the importance of D-loop nucleotides. Truncated 5′-oligonucleotides were synthesized and tested for their ability to stimulate aminoacylation of the 3′-59-mer. As shown in Figure 3A, six different deletion mutants were tested. The specificity constant (k_{cat}/K_M) of each mutant was determined and used to calculate the difference in the free energy of activation ($\Delta\Delta G^{\circ\ddagger}$) between the "wild-type" annealed fragment (assigned a k_{cat}/K_M of 1) and each mutant. These values are tabulated in Table 1. Surprisingly, a 5′-15-mer is better able to stimulate aminoacylation of the 3′-59-mer than the 18-mer (Table 1). The D-loop nucleotides U17a, U17, and C16 are apparently not essential for aminoacylation by ProRS. A substantial decrease in k_{cat}/K_M, however, is seen upon deletion of G15 ($-\Delta\Delta G^{\circ\ddagger}$ = 1.9 kcal/mol) and A14 ($-\Delta\Delta G^{\circ\ddagger}$ = 2.3 kcal/mol). Truncation of the 5′-strand to a 7-mer further reduced the level of charging ($-\Delta\Delta G^{\circ\ddagger}$ = 2.9 kcal/mol).

We wanted to assess whether the defect in stimulation by some of the truncated oligomers was due to incomplete annealing to the 3′-fragment. Since a duplex with a single-stranded overhang may have improved stability, a nonspecific 3′-UUU extension was added to the 13-mer to create the U3–

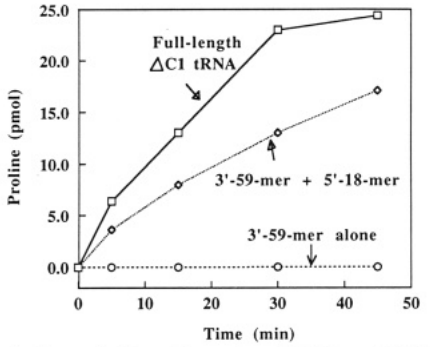

FIGURE 2: Aminoacylation with proline of full-length (ΔC1) *in vitro*-transcribed tRNA^{Pro} (4 μM), 3′-59 mer alone (4 μM), and annealed 5′-18-mer + 3′-59-mer (4 μM 3′-end). Assays were performed as described under Materials and Methods.

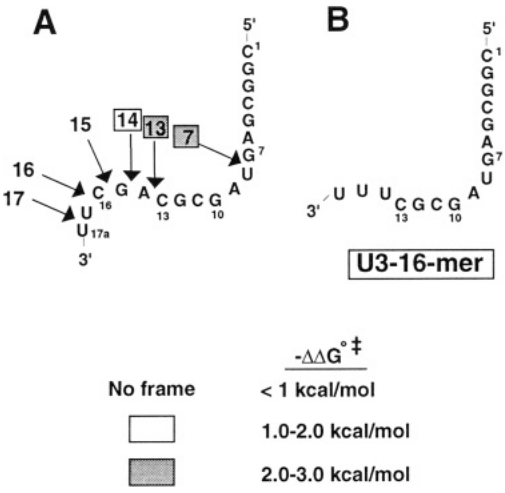

FIGURE 3: Variant RNA 5′-oligonucleotides prepared synthetically and tested for their ability to stimulate aminoacylation of the 3′-59-mer. (A) Truncated fragments tested. Numbered arrows indicate the length of each fragment from the 5′-end. (B) A 5′-16-mer fragment with the wild-type sequence from nucleotides 1–13 and a nonspecific 3′-UUU extension. ΔΔ*G* values were calculated as described in Table 1.

16-mer shown in Figure 3B. Although slightly increased levels of aminoacylation were achieved with this substrate ($-\Delta\Delta G^{\circ\ddagger}$ = 2.0 kcal/mol) relative to the 13-mer ($-\Delta\Delta G^{\circ\ddagger}$ = 2.3 kcal/mol), the relatively low levels of aminoacylation even in the presence of a 3′-overhang confirmed the functional significance of A14 and G15.

As a method of assessing whether the truncated oligomers were indeed annealing to the 3′-59-mer, the migration of the annealed tRNA molecules on a native polyacrylamide gel was compared to that of full-length ΔC1 tRNA^{Pro}. The native gel shown in Figure 4 compares the mobility of a full-length tRNA^{Pro} transcript (lane 1) to the separate 3′- and 5′-fragments (lanes 2 and 3) and to the annealed molecules (lanes 4–9). While the purified 3′-59-mer runs as two bands on a native gel presumably due to conformational flexibility (lane 2), these bands disappear in the lanes that correspond to the annealed substrates. Furthermore, a single band that comigrates with the full-length tRNA appears in the case of most of the annealed molecules shown in Figure 4. [The annealed 5′-13-mer + 3′-59-mer (lane 7) migrates as two species with very similar R_f values.] These results suggest that even the truncated fragments that show reduced levels of aminoacylation when combined with the 3′-fragment are able to anneal and stimulate folding of the 3′-3/4 tRNA molecule into a conformation that resembles the full-length tRNA molecule.

Single deoxy substitutions were introduced into nine positions of the 5′-18-mer (Figure 5). These changes were made to aid the interpretation of the experiments involving multiple deoxy substitutions (see below). In addition, these variants allowed us to probe the role of individual ribose 2′-hydroxyl groups in tRNA^{Pro} recognition by ProRS. In general, the single deoxy substitutions had relatively small effects on aminoacylation of the annealed substrates. The 2′-OH of G7 made the largest contribution to the free energy of transition state formation ($-\Delta\Delta G^{\circ\ddagger}$ = 0.98 kcal/mol). Slight increases in aminoacylation were actually seen for dG3, dG10, dC13, and dG15 variants (Table 1). In order to evaluate the possible involvement of G15 in a critical tertiary interaction, a single deoxyinosine substitution was made at this position (Figure 5). Inosine is a derivative of guanosine but lacks the 2-amino group. It forms a stable base pair with cytidine but has only two hydrogen bonds. Its incorporation into duplexes has been shown to have only minor effects on duplex stability, and so G to I substitutions test the role of the G 2-amino group (Musier-Forsyth & Schimmel, 1992; Case-Green & Southern, 1993). As indicated in Figure 5 and Table 1, a deoxyinosine substitution at position 15 resulted in a 3.7-fold decrease in k_{cat}/K_M. The fact that the single deoxy substitution at this position had no adverse effect (Table 1) suggests that the decrease seen with the deoxyinosine variant is due to the removal of the purine 2-amino group.

An all-DNA 5′-18 mer (Figure 6A) was also prepared and tested for its ability to stimulate charging of the 3′-59-mer. Interestingly, the all-DNA fragment failed to stimulate charging (Table 1). In order to determine if a specific domain of the annealed substrate was responsible for this result, the mixed 5′-oligonucleotides shown in Figure 6B–D were prepared. Multiple deoxy substitutions in the acceptor stem (5′-D5) and the D-loop (D-loop D3) were tolerated (Table 1). However, a variant containing four deoxynucleotides in the D-stem was a much poorer substrate (Figure 6C and Table 1). The 28-fold decrease in k_{cat}/K_M for this substrate is much greater than would have been predicted on the basis of the single deoxynucleotide substitutions. The effect of both multiple and single deoxynucleotide substitutions on the structure of the annealed tRNAs was assessed by native gel electrophoresis (Figure 7). The all-DNA (Figure 7A, lane 5) and D-stem D4 (Figure 7B, lane 9) substrates ran as smeared bands on a native gel rather than as a distinct band. This suggests that these 5′-oligomers are unable to combine with the 3′-fragment and fold into a single structure similar to full-length tRNA^{Pro} (Figure 7A, B, lane 1). On the other hand, all of the single deoxy-substituted variants and *active* multiple deoxy-substituted variants (Figure 7A, lanes 6–9, and Figure 7B, lanes 5–8) ran as single bands that comigrated with full-length tRNA^{Pro}.

DISCUSSION

Figure 8 shows an L-shaped representation of the *E. coli* tRNA^{Pro} isoacceptor used in this study. Hydrogen bonds that are predicted to play an important role in the tertiary folding of the tRNA are indicated by dotted lines. These interactions are based on the known three-dimensional structure of tRNA^{Phe} (Kim et al., 1974). Except for an extra nucleotide in the D-loop of tRNA^{Pro} (U17a), the length of these two tRNA sequences is identical. Proline tRNA is the only *E. coli* elongator tRNA with five nucleotides in the α-region of the D-loop. This is the portion of the D-loop preceding the two conserved G's at positions 18 and 19 and corresponds to A14 to U17a in tRNA^{Pro}. All other tRNAs have three or four nucleotides in this part of the D-loop. The precise effect of this structural difference on the hydrogen bonding interactions in the core region of the tRNA is not known.

Table 1: Relative Kinetic Parameters for Prolylation of Annealed $tRNA^{Pro}$ Molecules by *E. coli* Proline tRNA Synthetase[a]

5′-fragment	k_{cat}/K_M (relative)	change in specificity (*x*-fold)	$-\Delta\Delta G^{\circ\ddagger}$ (kcal/mol)	annealed
all-RNA				
18-mer	1	1	0	yes
17-mer	1	1	0	yes
16-mer	1	1	0	yes
15-mer	2.2	+2.2	–0.47	yes
14-mer	0.040	–24	1.9	yes
13-mer	0.020	–49	2.3	yes
7-mer	0.0072	–139	2.9	yes
U3-16-mer	0.035	–29	2.0	yes
single deoxy-substituted 18-mers				
dG2	0.75	–1.3	0.17	yes
dG3	1.7	+1.7	–0.31	yes
dG5	0.80	–1.2	0.13	yes
dG7	0.19	–5.3	0.98	yes
dG10	2.0	+2.0	–0.41	yes
dC11	0.24	–4.0	0.85	yes
dG12	0.55	–1.8	0.35	yes
dC13	1.1	+1.1	–0.057	yes
dG15	1.1	+1.1	–0.057	yes
dI15	0.27	–3.7	0.78	yes
multiple deoxy-substituted 18-mers				
all-DNA	0	–(>150)	>3.0	no
5′-D5	0.63	–1.6	0.27	yes
D-stem D4	0.036	–28	2.0	no
D-loop D3	0.85	–1.2	0.096	yes

[a] All 5′-fragments were chemically synthesized and annealed to 3′-59-mer fragments prepared by *in vitro* transcription. Initial rates of aminoacylation of these substrates were proportional to RNA concentration under the conditions employed for these experiments. This indicated that $V_0/[S]$ was an accurate reflection of k_{cat}/K_M. Determinations were made at three different substrate concentrations (1 μM, 2 μM, and 4 μM). The estimated error of these measurements was ±24%. In the cases where the loss in specificity was >5-fold, 5′-fragments were resynthesized, and the determination was repeated. $\Delta\Delta G^{\circ\ddagger}$ is the difference in the free energy of transition state formation between the "wild-type" substrate (all RNA 18-mer + 3′-59 mer) and the variants, and is given by $RT \ln(k_{cat}/K_M)^{variant}/(k_{cat}/K_M)^{wild\text{-}type}$. A "yes" indicates that the annealed fragments ran as a single band that comigrated with full-length $tRNA^{Pro}$ on a native gel. A "no" indicates that multiple bands were seen, and suggests the presence of several conformations.

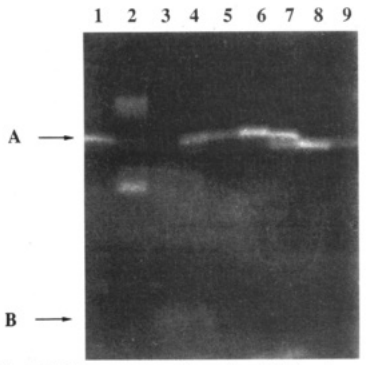

FIGURE 4: Ethidium-stained, native 12% polyacrylamide gel showing full-length *in vitro*-transcribed ΔC1 $tRNA^{Pro}$ (lane 1), 3′-59-mer alone (lane 2), 5′-18-mer RNA alone (lane 3), 3′-59-mer + 5′-18 mer (lane 4), +5′-15 mer (lane 5), +5′-14 mer (lane 6), +5′-13 mer (lane 7), +5′-7 mer (lane 8), and +5′-U3–16-mer (lane 9). Arrow A points to the position of full-length $tRNA^{Pro}$, and arrow B points to the position of the 5′-18-mer RNA oligonucleotide alone. The latter is not seen as a distinct band due to poor ethidium staining of short RNA oligonucleotides.

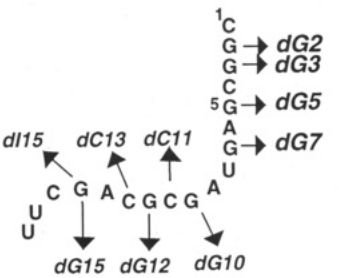

FIGURE 5: Ten single deoxyribonucleotide-containing 5′-18-mer fragments were prepared synthetically and tested for their ability to stimulate aminoacylation of the 3′-59-mer. Arrows point to the single site that was changed in each case. dI refers to deoxyinosine.

The symbols around certain nucleotides in Figure 8 highlight some of the positions probed using the fragment approach described in this paper. The deletion of U17a, U17, and C16 (Figure 8, open circles) in the D-loop had no effect on aminoacylation. Removal of G15 and A14 (Figure 8, shaded circles), on the other hand, had significant consequences. By truncating the 5′-oligonucleotide beyond position C16, nucleotides that are likely to be involved in tertiary interactions that stabilize the core of the tRNA structure are being deleted (Biou et al., 1994). These bases also serve to extend the stacking interactions of the D-stem by two base pairs (G15:C48 and U8:A14 in $tRNA^{Pro}$). The nucleotide at position 14 is a conserved adenosine in all nonmitochondrial elongator tRNAs, and is involved in a triple interaction with A21 and U8 in the known structure of $tRNA^{Phe}$. The nucleotide at position 15 of the D-loop is a semiconserved purine in all nonmitochondrial elongator tRNAs, and has been shown to make a tertiary interaction with a semiconserved pyrimidine at position 48 (Levitt, 1969). The crystal structure of yeast $tRNA^{Phe}$ shows that this base pair is a reverse Watson–Crick pair with only two hydrogen bonds involving the guanosine N1 and 2-NH_2 groups. To test the role of the 2-NH_2 group of G15, we prepared dG15 and dI15 mutants. Whereas a single deoxy change had no effect on aminoacylation, the dI15 mutant resulted in a 3.7-fold decrease in k_{cat}/K_M (Table 1, $-\Delta\Delta G^{\circ\ddagger} = 0.78$ kcal/mol). While this is less than the decrease seen upon G15 removal ($-\Delta\Delta G^{\circ\ddagger} = 1.9$ kcal/mol), it supports the involvement of the 2-amino group of G15 in an important tertiary interaction.

Each of the tRNA molecules prepared from a truncated 5′-fragment (Figure 3) folded into a conformation that comigrated with full-length $tRNA^{Pro}$ on a native polyacrylamide gel (Figure 4). However, gel electrophoresis is not a very sensitive probe of the subtle differences in tRNA structure that may be occurring as a result of the deletions. Chemicals that probe the tRNA tertiary structure and site-directed

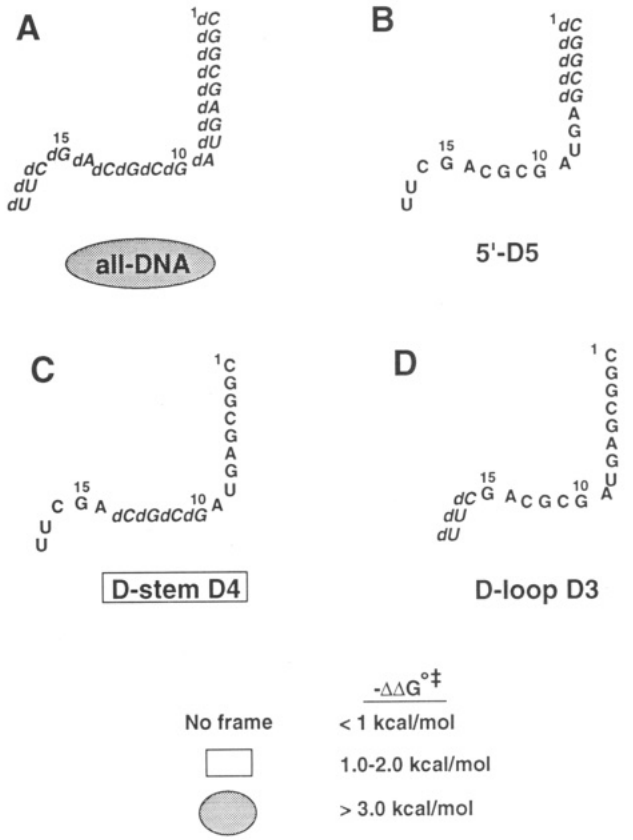

FIGURE 6: Mixed RNA–DNA 5′-oligonucleotides prepared synthetically and tested for their ability to stimulate aminoacylation of the 3′-59-mer. (A) An all-DNA 5′-18-mer. (B) A 5′-18-mer variant containing five deoxynucleotides at positions 1–5 of the acceptor stem ("5′-D5"). (C) A 5′-18-mer variant containing four deoxynucleotides at positions 10–13 of the D-stem ("D-stem D4"). (D) A 5′-18-mer variant containing three deoxynucleotides in the D-loop ("D-loop D3"). $\Delta\Delta G$ values were calculated as described in Table 1.

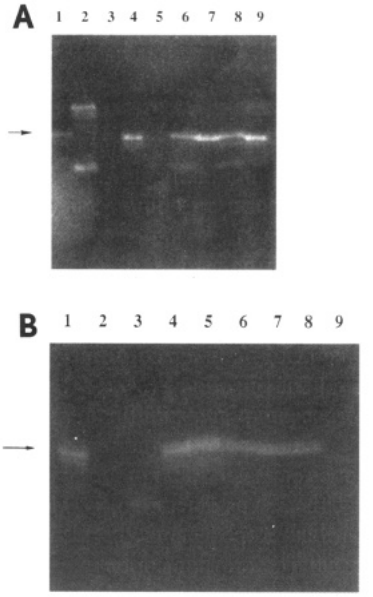

FIGURE 7: Ethidium-stained, native 12% polyacrylamide gels. *Panel A*: *In vitro*-transcribed ΔC1 tRNA^{Pro} (lane 1), 3′-59-mer alone (lane 2), 5′-18-mer RNA alone (lane 3), 3′-59-mer + 5′-RNA 18-mer (lane 4), +5′-DNA 18-mer (lane 5), +5′-dG2 18-mer (lane 6), +5′-dG3 18-mer (lane 7), +5′-dG5 18-mer (lane 8), and +"5′-D5" (lane 9). *Panel B*: *In vitro*-transcribed tRNA^{Pro} (lane 1), 5′-18-mer RNA alone (lane 2), 3′-59-mer alone (lane 3), 3′-59-mer + 5′-RNA 18-mer (lane 4), +5′-dG10 18-mer (lane 5), +5′-dC11 18-mer (lane 6), +5′-dG12 18-mer (lane 7), + 5′-dC13 18-mer (lane 8), +"D-stem D4"–18-mer (lane 9). The arrow points to the position of full-length tRNA^{Pro} in each gel.

mutagenesis of the full-length tRNA^{Pro} molecule are currently underway to further examine the functional and structural significance of these core interactions.

The effects of single and multiple deoxynucleotide substitutions were also examined in the context of the annealed substrate. Multiple deoxynucleotide substitutions in the first five positions of the acceptor helix of tRNA^{Pro} had only minor effects on aminoacylation efficiency (Figure 8, open rectangle). Apparently, the structural changes imposed by an RNA–DNA hybrid duplex in the acceptor helix of tRNA^{Pro} are tolerated by ProRS. Three of the single-stranded nucleotides in the D-loop (U17A, U17, and C16) could also simultaneously be changed to deoxynucleotides without a significant decrease in kinetic parameters (Table 1). However, ProRS was much more sensitive to changes that created a DNA–RNA hybrid helix in the D-stem (Figure 8, shaded rectangle). Theoretical (Sanghani & Lavery, 1994) and experimental (Roberts & Crothers, 1992; Ratmeyer et al., 1994) studies of hybrid duplexes support the notion that RNA–DNA hybrids have a conformation that is intermediate between a pure DNA and a pure RNA helix. The stability of hybrid duplexes and the degree to which they are more similar to either the A- or B-helical forms appear to be sequence-dependent (Ratmeyer et al., 1994). Recent circular dichroism and gel electrophoresis experiments, however, suggest that mixed purine–pyrimidine sequences such as the sequence in the D-stem of tRNA^{Pro} are likely to have truly intermediate conformations (Ratmeyer et al., 1994). In our studies, native gel electrophoresis indicated that the four deoxynucleotides in the D-stem prevented the tRNA molecule from folding into a single predominant conformation (Figure 7B, lane 9). Individual deoxynucleotide substitutions at the same four positions did not have an effect on global folding (Figure 7B, lanes 5–8) and only a minor effect on activity (Table 1), suggesting a cooperative effect of these changes in the quadruple mutant. The fact that D-stem stability is coupled to the presence of interactions in the core of the tRNA has been previously demonstrated (Coutts et al., 1974; Crothers et al., 1974; Puglisi et al., 1993). The sensitivity of ProRS to D-stem helical conformation suggests that the decreases in aminoacylation upon removal of G15 and A14 (see above) may be due to an indirect effect of these deletions on D-stem structure.

Clearly, the rules that define tRNA recognition by cognate aminoacyl-tRNA synthetases are complex. The recognition of specific chemical groups and the correct presentation of these functional groups to the enzymes both appear to be important. The acceptor stem and anticodon loop have been shown to contain major recognition elements for specific aminoacylation of ProRS *in vivo* (McClain et al., 1994) and *in vitro* (H. Liu, J. Kessler, R. Peterson, and K. Musier-Forsyth, unpublished results). Moreover, a footprinting analysis using iodine cleavage of phosphorothioate-containing tRNA^{Pro} transcripts (Schatz et al., 1991) shows that major sites of phosphate protection are located in the acceptor and anticodon stems (B. Ostlie and K. Musier-Forsyth, unpublished results). The present study clearly demonstrates the important role of structural elements outside of the acceptor stem and anticodon loop in tRNA^{Pro} aminoacylation *in vitro*. ProRS is particularly sensitive to changes that disrupt the helical conformation of the D-stem in the core of the tRNA molecule.

A minihelix corresponding to the acceptor–TΨC domain of tRNA^{Pro} is not a good substrate for ProRS. Furthermore, unlike the valine-specific system (Frugier et al., 1992), the aminoacylation of minihelix^{Pro} cannot be stimulated by a separate anticodon stem-loop domain (H. Liu and K. Musier-Forsyth, unpublished results). Therefore, presenting ProRS

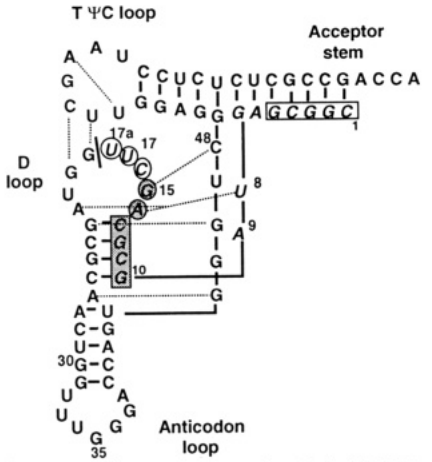

FIGURE 8: Summary of experiments using hybrid RNA–DNA and truncated 5′-oligonucleotides. *Open circles* have been placed around nucleotides that could be deleted without reducing the aminoacylation efficiency. A significant reduction in aminoacylation occurred upon deletion of nucleotides indicated by *shaded circles*. The *open rectangle* indicates nucleotides that could simultaneously be changed to deoxynucleotides without significant loss in activity. When all four positions indicated by the *shaded rectangle* were simultaneously changed to deoxynucleotides, a significant decrease in aminoacylation was seen. The dotted lines represent probable tertiary interactions and are based on the known structure of $tRNA^{Phe}$.

with important recognition elements in the absence of the framework that normally ties them together is not sufficient for aminoacylation by ProRS. The L-shape tRNA architecture is apparently required for the correct presentation of the recognition elements and for information transfer between distal regions of the tRNA molecule.

An active $tRNA^{Pro}$ molecule can also be assembled by annealing fragments that result in a break in the TΨC loop (L. Yap and K. Musier-Forsyth, unpublished result). Truncated 3′-oligomers are being tested for their ability to be aminoacylated in the presence of a 5′-3/4 tRNA molecule. These experiments should lead to additional insights into the structure–function relationship of $tRNA^{Pro}$ recognition by ProRS and into RNA–protein interactions in general.

ACKNOWLEDGMENT

We thank Dr. Mike Syvaney for providing us with the overexpression plasmid for ProRS, and gratefully acknowledge Dr. F. William Studier for the gift of the overexpression plasmid for T7 RNA polymerase. We also thank Dr. Christopher Francklyn, Dr. Paul Siliciano, and Ms. LiPing Yap for critical reading and helpful comments on the manuscript.

REFERENCES

Biou, V., Yaremchuk, A., Tukalo, M., & Cusack, S. (1994) *Science 263*, 1404–1410.

Case-Green, S. C., & Southern, E. M. (1993) *Nucleic Acids Res. 22*, 131–136.

Chow, C. S., & Barton, J. K. (1990) *J. Am. Chem. Soc. 112*, 2839–2841.

Chow, C. S., & Barton, J. K. (1992) *Biochemistry 31*, 5423–5429.

Chow, C. S., Behlen, L. S., Uhlenbeck, O. C., & Barton, J. K. (1992) *Biochemistry 31*, 972–982.

Coutts, S. M., Gangloff, J., & Dirheimer, G. (1974) *Biochemistry 13*, 3938–3948.

Crothers, D. M., Cole, P. E., Hilbers, C. W., & Schulman, R. G. (1974) *J. Mol. Biol. 87*, 63–88.

Cusack, S., Berthet-Colominas, C., Härtlein, M., Nassar, N., & Leberman, R. (1990) *Nature 347*, 249–265.

Eriani, G., Delarue, M., Poch, O., Gangloff, J., & Moras, D. (1990) *Nature 347*, 203–206.

Fersht, A. R., Ashford, J. S., Bruton, C. J., Jakes, R., Koch, G. L. E., & Hartley, B. S. (1975) *Biochemistry 14*, 1–4.

Fittler, F., & Zachau, H. G. (1973) *Arch. Biochem. Biophys. 155*, 368–380.

Frugier, M., Florentz, C., & Giegé, R. (1992) *Proc. Natl. Acad. Sci. U.S.A. 89*, 3990–3994.

Giegé, R., Puglisi, J. D., & Florentz, C. (1993) *Prog. Nucleic Acid Res. Mol. Biol. 45*, 129–205.

Grodberg, J. D., & Dunn, J. J. (1988) *J. Bacteriol. 170*, 1245–1253.

Hayase, Y., Jahn, M., Rogers, M. J., Sylvers, L. A., Koizumi, M., Inoue, H., & Söll, D. (1992) *EMBO J. 11*, 4159–4165.

Holmes, C. E., Carter, B. J., & Hecht, S. M. (1993) *Biochemistry 32*, 4293–4307.

Hou, Y.-M. (1994) *Biochemistry 33*, 4677–4681.

Hou, Y.-M., Westhof, E., & Giegé, R. (1993) *Proc. Natl. Acad. Sci. U.S.A. 90*, 6776–6780.

Imura, N., Weiss, G. B., & Chambers, R. W. (1969) *Nature (London) 222*, 1147–1148.

Jasin, M., Regan, L., & Schimmel, P. (1985) *J. Biol. Chem. 260*, 2226–2230.

Kim, S. H., Suddath, F. L., Quigley, G. J., McPherson, A., Sussman, J. L., Wang, A. H. J., Seeman, N. C., & Rich, A. (1974) *Science 185*, 435–440.

Levitt, M. (1969) *Nature 224*, 759–763.

McClain, W. H. (1993) *J. Mol. Biol. 234*, 257–280.

McClain, W. H., Schneider, J., & Gabriel, K. (1994) *Nucleic Acids Res. 22*, 522–529.

Milligan, J. R., Groebe, D. R., Witherell, G. W., & Uhlenbeck, O. C. (1987) *Nucleic Acids Res. 15*, 8783–8798.

Musier-Forsyth, K., & Schimmel, P. (1992) *Nature 357*, 513–515.

Musier-Forsyth, K., Scaringe, S., Usman, N., & Schimmel, P. (1991) *Proc. Natl. Acad. Sci. U.S.A. 88*, 209–213.

Perret, V., Florentz, C., Puglisi, J. D., & Giegé, R. (1990) *J. Mol. Biol. 226*, 323–333.

Peterson, E. T., & Uhlenbeck, O. C. (1992) *Biochemistry 31*, 10380–10389.

Puglisi, J. D., Pütz, J., Florentz, C., & Giegé, R. (1993) *Nucleic Acids Res. 21*, 41-49.

Pütz, J., Puglisi, J. D., Florentz, C., & Giegé, R. (1993) *EMBO J. 12*, 2949–2957.

Ratmeyer, L., Vinayak, R., Zhong, Y. Y., Zon, G., & Wilson, W. D. (1994) *Biochemistry 33*, 5298–5304.

Roberts, W. R., & Crothers, D. M. (1992) *Science 258*, 1463–1466.

Saks, M. E., Sampson, J. R., & Abelson, J. N. (1994) *Science 263*, 191–197.

Sampson, J. R., & Uhlenbeck, O. C. (1988) *Proc. Natl. Acad. Sci. U.S.A. 85*, 1033–1037.

Sampson, J. R., DiRenzo, A. B., Behlen, L. S., & Uhlenbeck, O. C. (1990) *Biochemistry 29*, 2523–2532.

Sanghani, S. R., & Lavery, R. (1994) *Nucleic Acids Res. 22*, 1444–1449.

Scaringe, S. A., Francklyn, C., & Usman, N. (1990) *Nucleic Acids Res. 18*, 5433–5441.

Schatz, D., Leberman, R., & Eckstein, F. (1991) *Proc. Natl. Acad. Sci. U.S.A. 88*, 6132–6136.

Schimmel, P. (1987) *Annu. Rev. Biochem. 56*, 125–158.

Shi, J.-P., Francklyn, C., Hill, K., & Schimmel, P. (1990) *Biochemistry 29*, 3621–3626.

Sprinzl, M., Hartmann, T., Weber, J., Blank, J., & Zeidles, R. (1989) *Nucleic Acids Res. 17*, r1–r172.

Thiebe, R., & Zachau, H. G. (1969) *Biochem. Biophys. Res. Commun. 36*, 1024–1031.

Thiebe, R., Harbers, K., & Zachau, H. G. (1972) *Eur. J. Biochem. 26*, 144–152.

Wübbeler, W., Lossow, C., Fittler, F., & Zachau, H. G. (1975) *Eur. J. Biochem. 59*, 405–413.